ELECTRONIC SUPPORTING INFORMATION

Peripheral site modification in a family of dinuclear [Dy$_2$(hynad)$_{2-6}$(NO$_3$)$_{0-6}$(sol)$_{0-2}$]$^{0/2-}$ single-molecule magnets bearing a {Dy$_2$(µ-OR)$_2$}$^{4+}$ diamond-shaped core and exhibiting dissimilar magnetic dynamics

Alexandros S. Armenis,[†] Dimitris I. Alexandropoulos,[‡] Anne Worrell,[⌂] Luís Cunha-Silva,[◊] Kim R. Dunbar,[‡] and Theocharis C. Stamatatos*,[†,#]

[†] Department of Chemistry, University of Patras, 26504 Patras, Greece. E-mail: thstama@upatras.gr; Tel: +30 2610 996730.

[‡] Department of Chemistry, Texas A&M University, College Station, Texas 77843, USA.

[⌂] Department of Chemistry, 1812 Sir Isaac Brock Way, Brock University, L2S 3A1 St. Catharines, Ontario, Canada

[◊] LAQV/REQUIMTE & Department of Chemistry and Biochemistry, Faculty of Sciences, University of Porto, 4169-007 Porto, Portugal

[#] Institute of Chemical Engineering Sciences, Foundation for Research and Technology – Hellas (FORTH/ICE – HT), Platani, P.O. Box 1414, 26504, Patras, Greece

Table S1. Crystallographic data for compounds **1-4**.

Parameter	1	2·2MeCN	3·2DMF	4·2DMF
Formula	$C_{30}H_{26}Dy_2N_8O_{20}$	$C_{36}H_{42}Dy_2N_{12}O_{24}$	$C_{54}H_{42}Dy_2N_8O_{22}$	$C_{78}H_{54}Dy_2N_8O_{22}$
F_w / g·mol^{-1}	1143.59	1351.81	1479.95	1780.29
Crystal system	Triclinic	Triclinic	Triclinic	Triclinic
Space group	$P\bar{1}$	$P\bar{1}$	$P\bar{1}$	$P\bar{1}$
a / Å	9.7495(3)	10.9643(3)	10.8846(5)	12.1938(8)
b / Å	10.3059(3)	11.4838(3)	12.5023(6)	12.3905(8)
c / Å	10.8266(2)	11.7527(5)	14.2375(6)	14.0035(9)
α / °	91.834(2)	115.252(3)	64.886(4)	94.080(3)
β / °	112.263(2)	109.857(3)	84.877(3)	93.689(3)
γ / °	112.030(3)	96.441(2)	76.325(4)	94.619(3)
V / Å^3	913.81(5)	1199.95(8)	1704.45(15)	2098.3(2)
Z	1	1	1	1
T / K	173.0(1)	173.0(1)	150(2)	150(2)
Radiation / μ (mm^{-1})	Cu Kα / 22.497	Cu Kα / 17.337	Cu Kα / 12.224	Mo Kα / 1.840
ρ_{calcd} / g cm^{-3}	2.078	1.871	1.442	1.409
Reflections collected/unique (R_{int})	8071/3221 (0.0344)	7372/4225 (0.0446)	15758/5965 (0.0632)	62031/7395 (0.0602)
Reflections with $I>2\sigma(I)$	3037	3823	5288	6965
No. of parameters	273	339	427	453
R_1 [$I>2\sigma(I)$], wR_2 [$I>2\sigma(I)$]^{a,b}	0.0241, 0.0570	0.0282, 0.0651	0.0460, 0.1325	0.0714, 0.2009
R_1 (all data), wR_2 (all data)^{a,b}	0.0288, 0.0596	0.0369, 0.0696	0.0567, 0.1606	0.0750, 0.2032
$(\Delta/\sigma)_{max}$	0.001	0.001	0.000	0.002
$\Delta\rho_{max}/\Delta\rho_{min}$ (e Å^{-3})	0.759 / -0.388	0.580 / -0.740	0.867 / -1.197	3.393, -2.629
CCDC number	2278244	2278245	2278246	2278247

^{a} $R_1 = \Sigma(|F_o| - |F_o|) / \Sigma(|F_o|)$.

^{b} $wR_2 = \{\Sigma[w(F_o^2 - F_c^2)^2] / \Sigma[w(F_o^2)^2]\}^{1/2}$, $w = 1 / [\sigma^2(F_o^2) + (aP)^2 + bP]$, where $P = [max(F_o^2, 0) + 2 F_c^2] / 3$.

Table S2. Selected bond distances (Å) and angles (°) for complex **1**.

Bond distances (Å)	
Dy1-O1	2.286(2)
Dy1-O2	2.445(3)
Dy1-O4	2.476(4)
Dy1-O5	2.486(3)
Dy1-O6	2.456(2)
Dy1-O8	2.331(2)
Dy1-O8′	2.332(3)
Dy1-O9	2.430(2)
Dy1-O10′	2.456(2)
Bond angles (°)	
O1-Dy1-O10′	90.8(9)
O1-Dy1-O9	80.9(0)
O9-Dy1-O8	65.3(7)
O8′-Dy1-O8	60.9(9)
O8-Dy1-O10′	64.5(4)

Symmetry code: (′) -x, -y, -z.

Table S3. Selected bond distances (Å) and angles (°) for complex **2**·2MeCN.

Bond distances (Å)	
Dy1-O1	2.441(2)
Dy1-O2′	2.364(2)
Dy1-O2	2.377(2)
Dy1-O3′	2.469(2)
Dy1-O4	2.433(3)
Dy1-O5	2.518(3)
Dy1-O7	2.452(3)
Dy1-O8	2.575(3)
Dy1-O10	2.426(3)

Dy1-O12	2.516(3)
Bond angles (°)	
O2-Dy1-O3′	64.1(1)
O2-Dy1-O2′	58.8(1)
O2-Dy1-O1	64.3(1)
O1-Dy1-O8	64.9(1)
O8-Dy1-O7	50.2(1)
O7-Dy1-O3	67.6(1)

Symmetry code: (′) -*x*, -*y*, -*z*.

Table S4. Selected bond distances (Å) and angles (°) for complex **3**·2DMF.

Bond distances (Å)	
Dy1-O2	2.362(4)
Dy1-O2′	2.417(4)
Dy1-O4	2.396(4)
Dy1-O1	2.507(5)
Dy1-O5	2.332(4)
Dy1-O7	2.535(5)
Dy1-O8	2.483(5)
Dy1-O3′	2.442(5)
Dy1-O1W	2.480(5)
Bond angles (°)	
O2-Dy1-O1	64.0(2)
O1-Dy1-O4	80.4(2)
O4-Dy1-O3	84.1(2)
O3-Dy1-O2	64.0(2)
O2-Dy1-O2′	62.1(2)
O8-Dy1-O7	50.3(2)
O4-Dy1-O5	65.7(2)

Symmetry code: (′) -*x*, -*y*, -*z*.

Table S5. Selected bond distances (Å) and angles (°) for complex **4**·2DMF.

Bond distances (Å)	
Dy1-O1	2.384(6)
Dy1-O1′	2.447(6)
Dy1-O2′	2.509(6)
Dy1-O3	2.522(7)
Dy1-O4	2.436(7)
Dy1-O5	2.309(7)
Dy1-O7	2.337(6)
Dy1-O8	2.443(7)
Dy1-O11	2.429(7)
Bond angles (°)	
O1-Dy1-O3	63.8(2)
O3-Dy1-O8	67.3(2)
O8-Dy1-O2′	91.9(2)
O2-Dy1-O1	63.0(2)
O7-Dy1-O8	65.6(2)
O4-Dy1-O5	66.0(2)
O1-Dy1-O1′	62.4(2)

Symmetry code: (′) -*x*, -*y*, -*z*.

Table S6. Continuous Shape Measures (CShM) values for the potential coordination polyhedra of the 9-coordinate Dy^{III} centers in the structures of complexes **1**, **3**·2DMF and **4**·2DMF.

Polyhedron[a,b]	Dy1 / Dy1′ (1)	Dy1 / Dy1′ (3)	Dy1 / Dy1′ (4)
EP	35.25	31.63	32.78
OPY	23.54	23.37	23.8
HBPY	14.91	15.33	17.42
JTC	14.8	13.88	15.50
JCCU	8.32	7.56	7.00
CCU	6.47	6.23	5.75
JCSAPR	4.79	5.02	3.14
CSAPR	3.52	4.06	2.25
JTCTPR	6.27	4.26	2.99
TCTPR	4.53	4.00	**2.05**
JTDIC	9.8	10.68	12.29
HH	6.87	5.32	7.60
MFF	**2.73**	**3.29**	2.49

[a] Abbreviations: EP, Enneagon; OPY, Octagonal pyramid; HBPY, Heptagonal bipyramid; JTC, Johnson triangular cupola; JCCU, Capped cube; CCU, Spherical-relaxed capped cube; JCSAPR, Capped square antiprism, CSAPR-9, Spherical capped square antiprism; JTCTPR, Tricapped trigonal prism; TCTPR, Spherical tricapped trigonal prism; JTDIC, Tridiminished icosahedron, HH, Hula-hoop; MFF, Muffin. [b] The values in boldface indicate the closest polyhedron according to the Continuous Shape Measures.

Table S7. Continuous Shape Measures (CShM) values for the potential coordination polyhedra of the 10-coordinate Dy^{III} centers in the structure of complex **2**·2MeCN

Polyhedron[a,b]	Dy1 / Dy1′ (2)
DP	35.25
EPY	25.28
OBPY	16.41
PPR	11.48
PAPR	10.78
JBCCU	9.03
JBCSAPR	4.51
JMBIC	6.46
JATDI	18.12
JSPC	3.55
SDD	3.12
TD	**2.24**
HD	6.06

[a] Abbreviations: DP, Decagon; EPY, Enneagonal pyramid; OBPY, Octagonal bipyramid; PPR, Pentagonal prism; PAPR, Pentagonal antiprism; JBCCU, Bicapped cube; JBCSAPR, Bicapped square antiprism; JMBIC, Metabidiminished icosahedron; JATDI, Augmented tridiminished icosahedron; JSPC, Sphenocorona; SDD, Staggered dodecahedron; TD, Tetradecahedron; HD, Hexadecahedron. [b] The value in boldface indicates the closest polyhedron according to the Continuous Shape Measures.
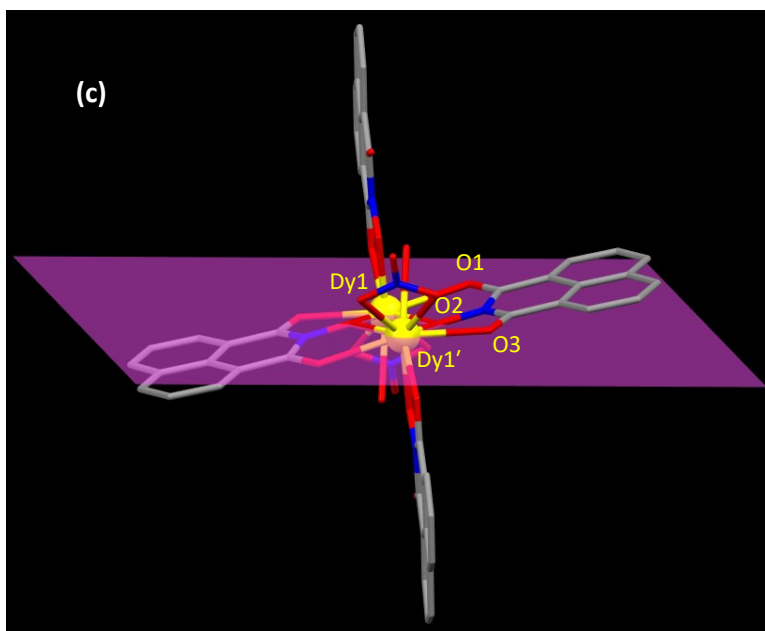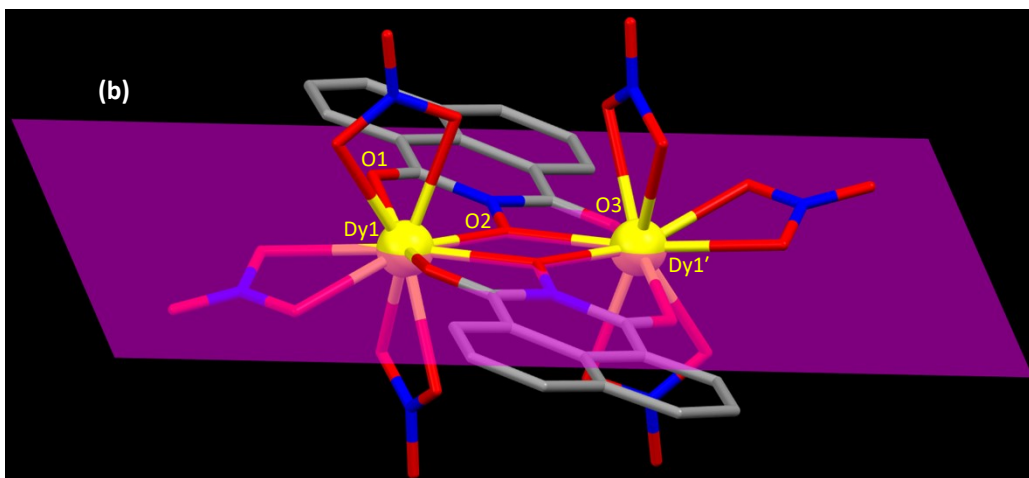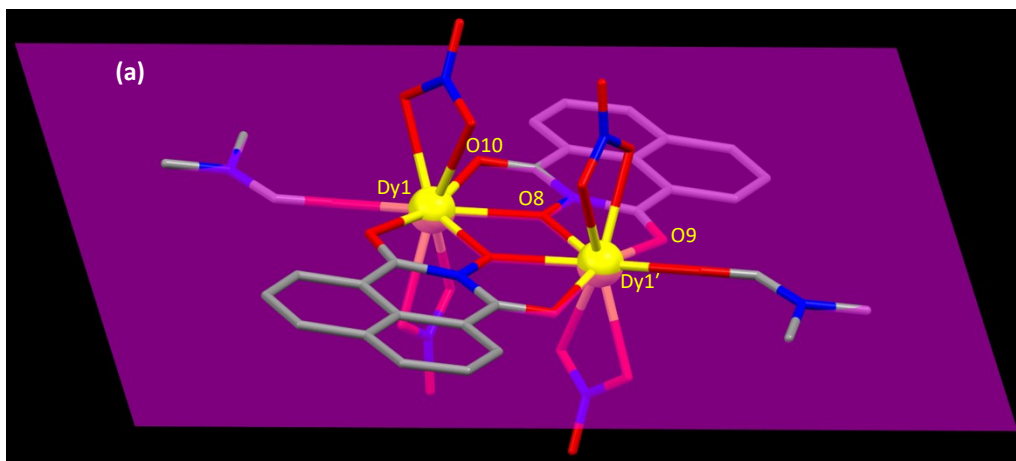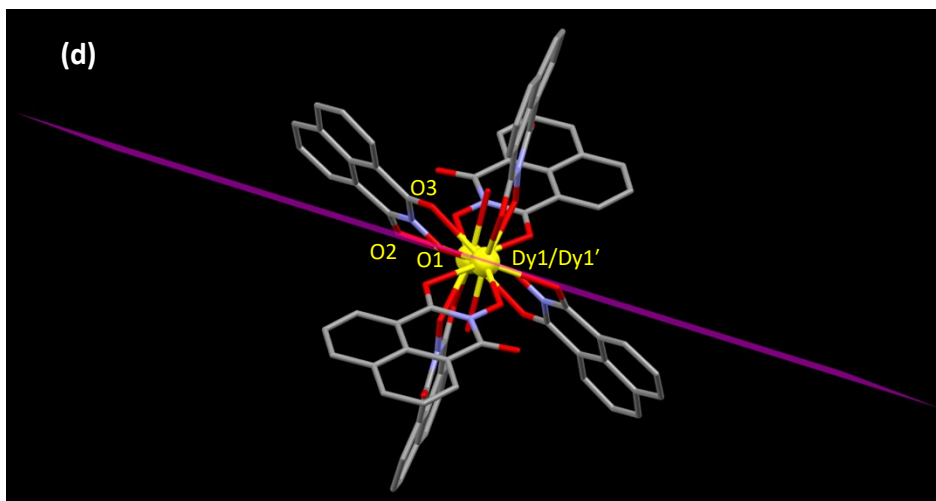
Figure S1. Bridging hynad⁻ ligands' twist with respect to the central, planar {Dy₂O₂} core (highlighted with magenta) in complexes **1** (a), **2** (b), **3** (c), and **4** (d); see the text for the corresponding discussion. Color scheme: Dy^{III}, yellow; O, red; N, blue; C, grey. H-atoms are omitted for clarity.
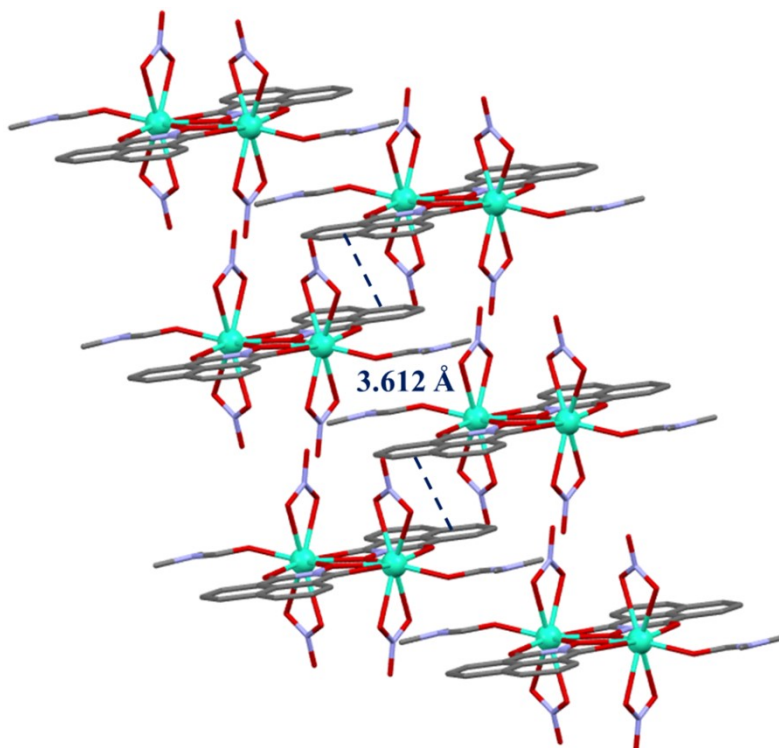

Figure S2. A portion of the repeating dimers in the crystal of **1** and their interactions with their neighboring units through strong π–π stacking interactions (dark blue dashed lines) along the *c*-axis. The Dy^{III} ions are illustrated as cyan spheres.
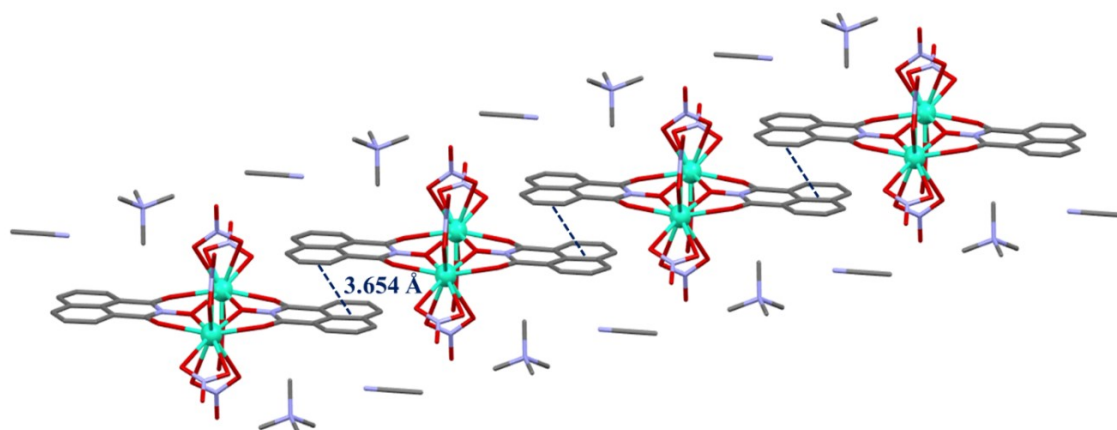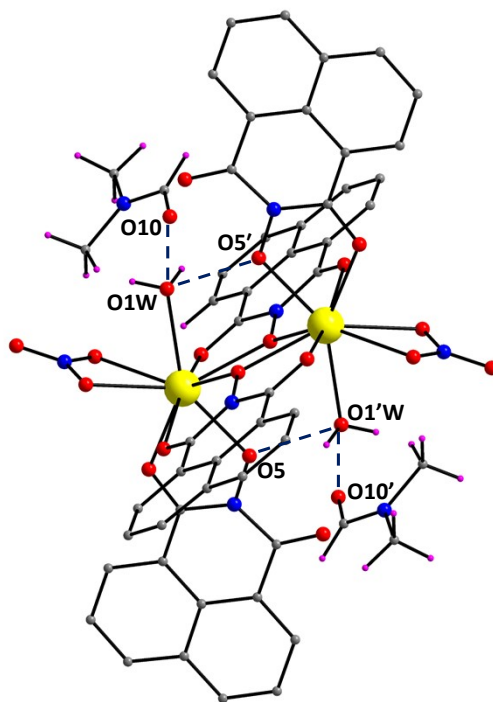
Figure S3. A portion of the repeating dimers in the crystal of **2**·2MeCN (including lattice solvents and countercations), and their interactions with their neighboring units through strong π–π stacking interactions (dark blue dashed lines) along the *b*-axis. The Dy^{III} ions are illustrated as cyan spheres.

Figure S4. Structure of **3**·2DMF showing the intramolecular hydrogen bonding interactions (dark blue dashed lines); see the text for the corresponding discussion. Color scheme: Dy^{III}, yellow; O, red; N, blue; C, grey; H, magenta.
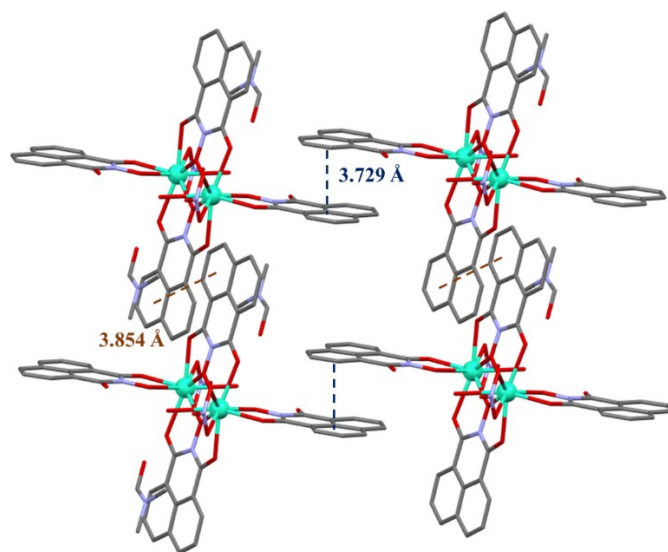
Figure S5. A portion of the repeating dimers in the crystal of **3**·2DMF (including lattice solvents), and their interactions with their neighboring units through π–π stacking interactions along the *c*- (dark blue dashed lines) and *a*-axes (brown dashed lines). The Dy^{III} ions are illustrated as cyan spheres.
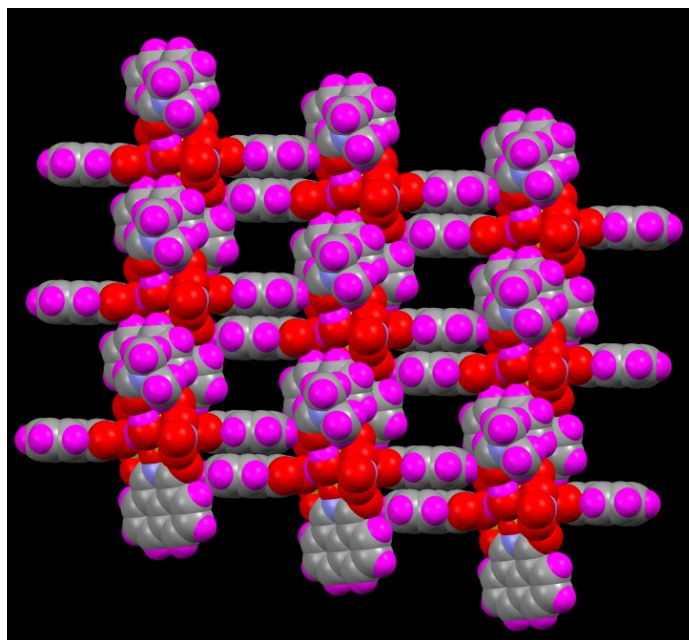

Figure S6. A small portion of the 2-D porous framework created by the strong intermolecular π-π stacking interactions between neighboring {Dy$_2$} molecules in the crystal of **3**·2DMF. Color scheme: Dy^{III}, yellow; O, red; N, blue; C, grey; H, magenta.
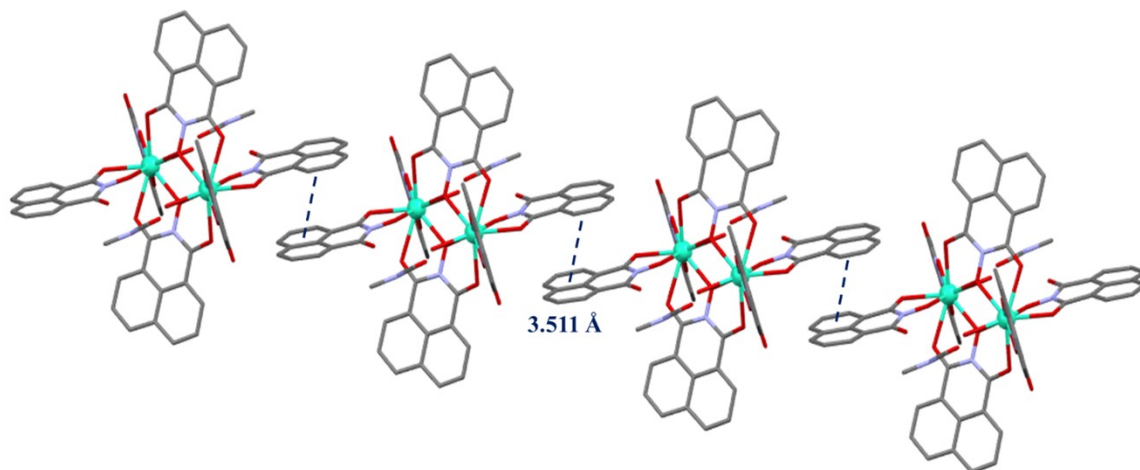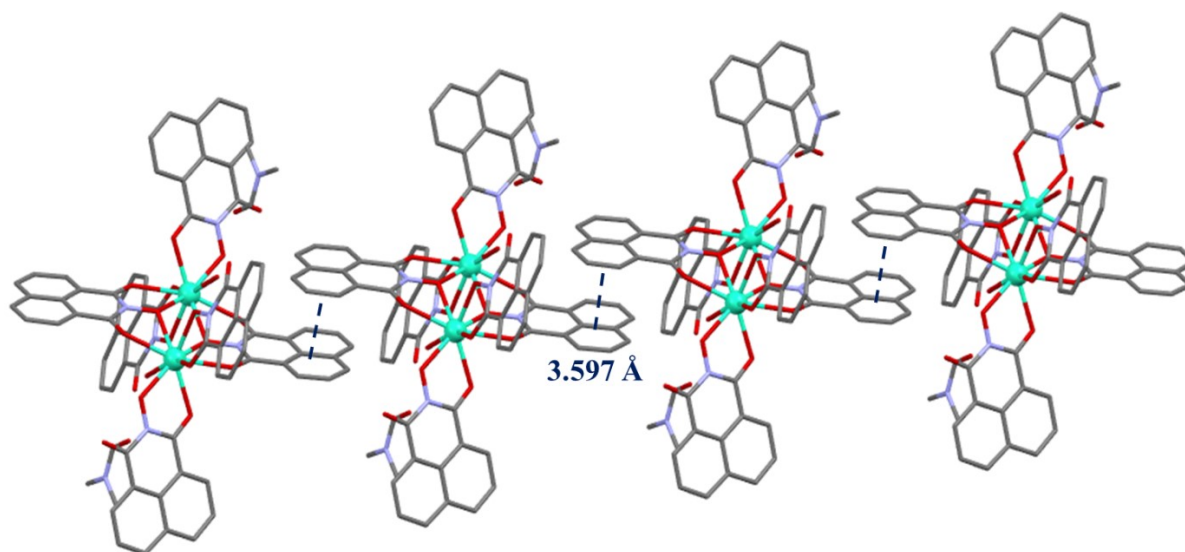
Figure S7. A portion of the repeating dimers in the crystal of **4**·2DMF (including lattice solvents), and their interactions with the neighboring units through strong π–π stacking interactions (dark blue dashed lines) along the *c*-axis. The Dy^{III} ions are illustrated as cyan spheres.

Figure S8. A portion of the repeating dimers in the crystal of **4**·2DMF (including lattice solvents), and their interactions with the neighboring units through strong π–π stacking interactions (dark blue dashed lines) along the *a*-axis. The Dy^{III} ions are illustrated as cyan spheres.
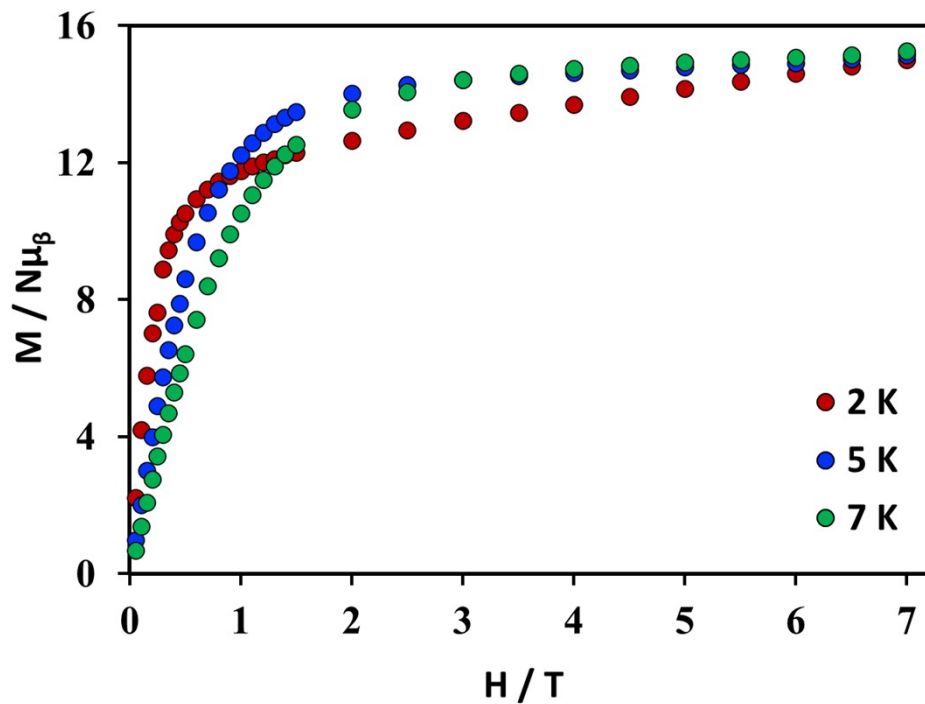
Figure S9. Plots of magnetization (*M*) vs field (*H*) for complex **1** at three different low temperatures.
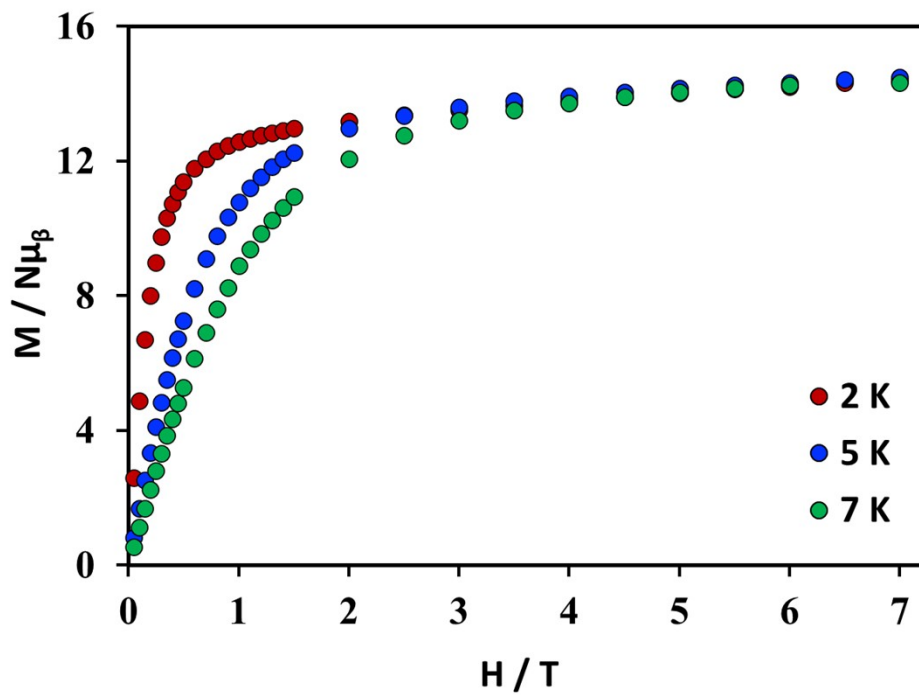

Figure S10. Plots of magnetization (*M*) vs field (*H*) for complex **2** at three different low temperatures.
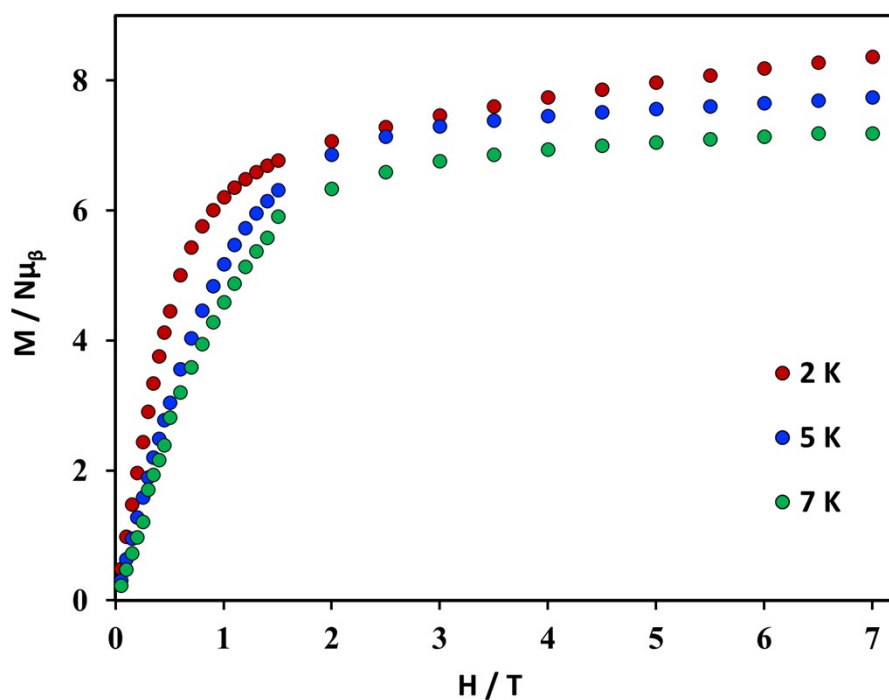
Figure S11. Plots of magnetization (*M*) vs field (*H*) for complex **3** at three different low temperatures.
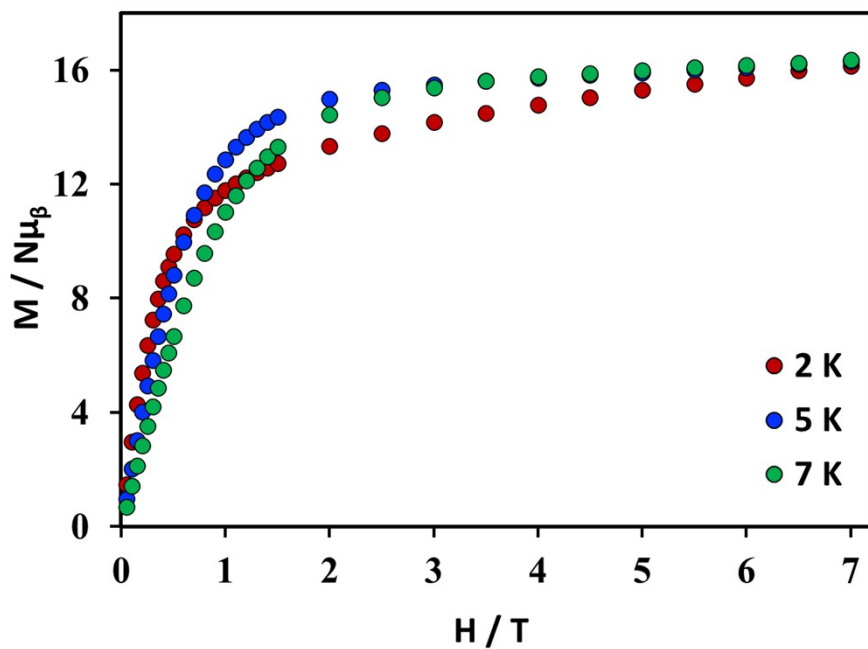

Figure S12. Plots of magnetization (*M*) vs field (*H*) for complex **4** at three different low temperatures.

Figure S13. Cole−Cole plot for complex **1** obtained using the *ac* susceptibility data in zero applied *dc* field at the temperature range 1.8-5.7 K. The solid lines correspond to the best fit obtained with a generalized Debye model (see the text for the fit parameters).
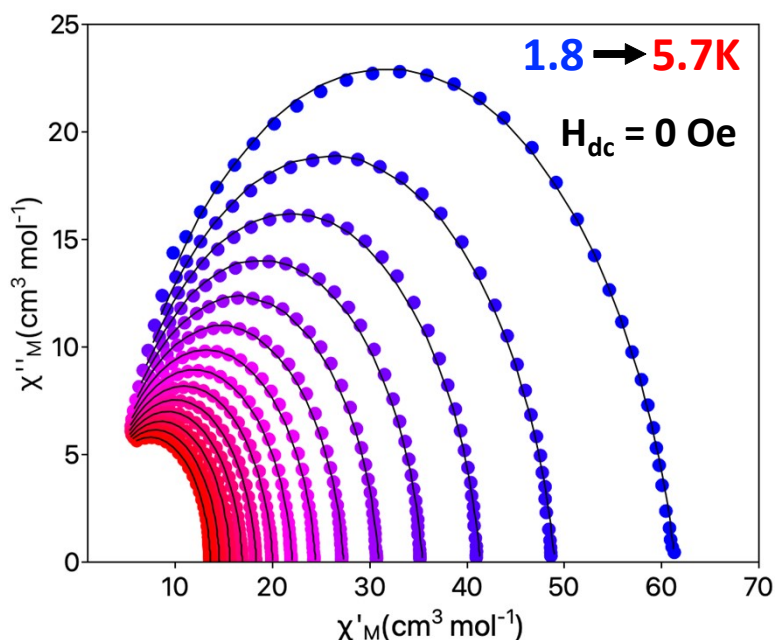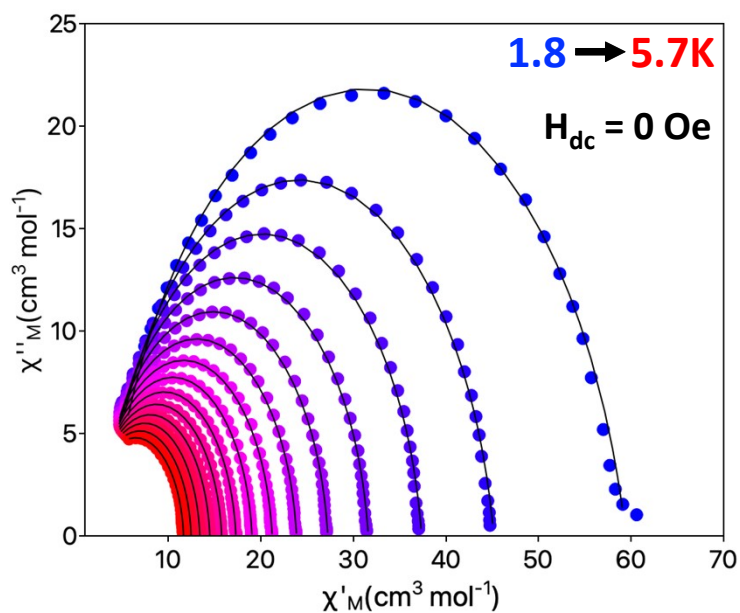

Figure S14. Cole−Cole plot for complex **2** obtained using the *ac* susceptibility data in zero applied *dc* field at the temperature range 1.8-5.7 K. The solid lines correspond to the best fit obtained with a generalized Debye model (see the text for the fit parameters).
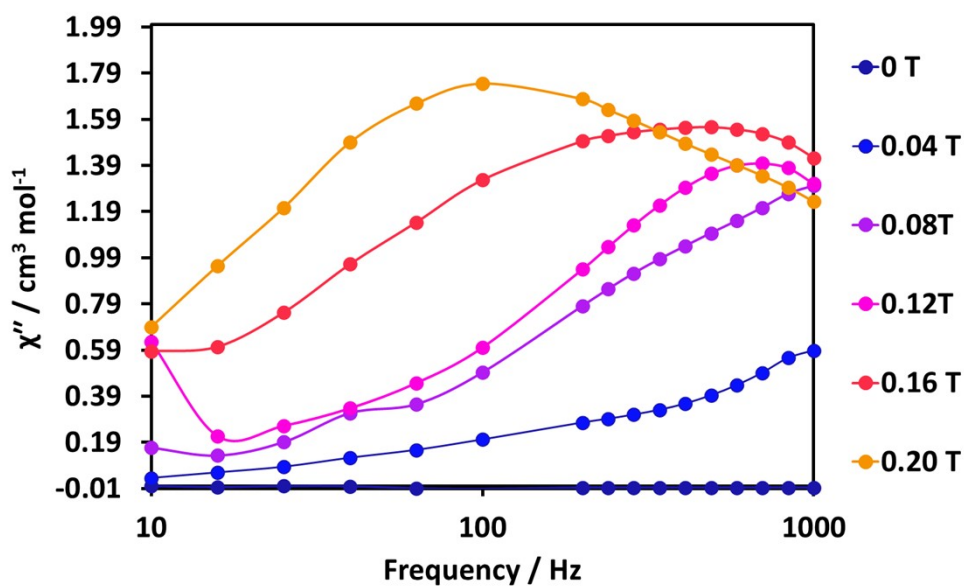
Figure S15. Field dependence of the out-of-phase magnetic susceptibility (χ'') vs frequency for complex **3** at 2 K.
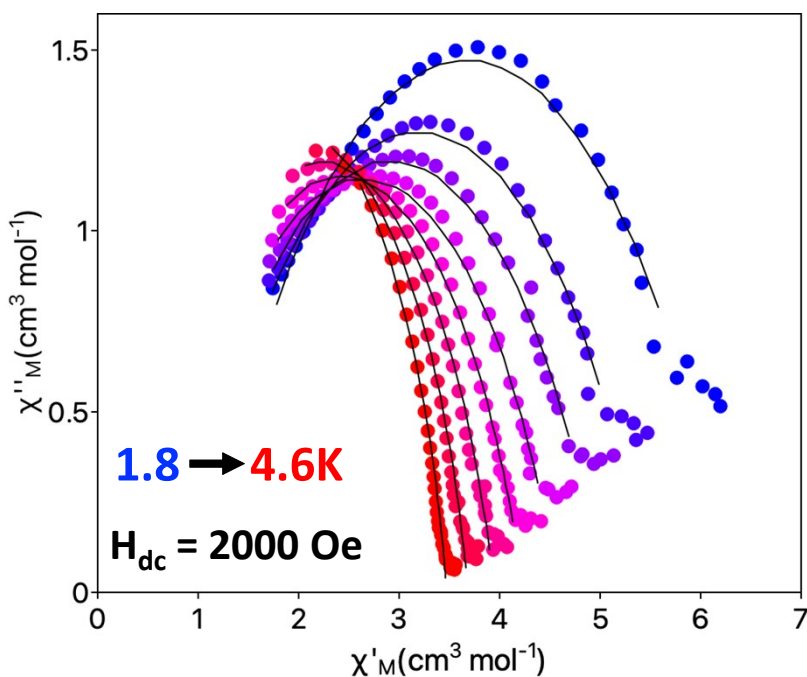
Figure S16. Cole−Cole plot for complex **3** obtained using the *ac* susceptibility data in 2000 Oe applied *dc* field at the temperature range 1.8-4.6 K. The solid lines correspond to the best fit obtained with a generalized Debye model (see the text for the fit parameters).
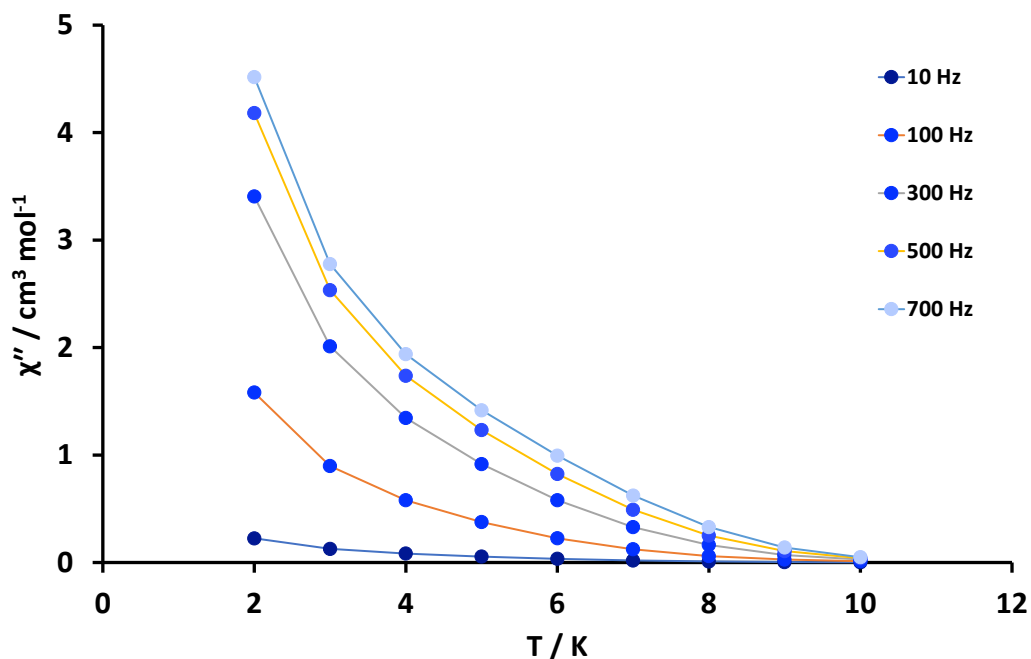
Figure S17. Temperature dependence of the out-of-phase (χ_M'') *ac* magnetic susceptibility in zero *dc* field for **4**, measured in a 3.0 G *ac* field oscillating at the indicated frequencies. The solid lines are guides only.

Figure S18. Field dependence of the out-of-phase magnetic susceptibility (χ'') vs frequency for complex **4** at 2 K.

Figure S19. Cole−Cole plot for complex **4** obtained using the *ac* susceptibility data under an 800 Oe applied *dc* field over the temperature range 2.0-8.5 K. The solid lines correspond to the best fit obtained with a generalized Debye model (see the text for the fit parameters).
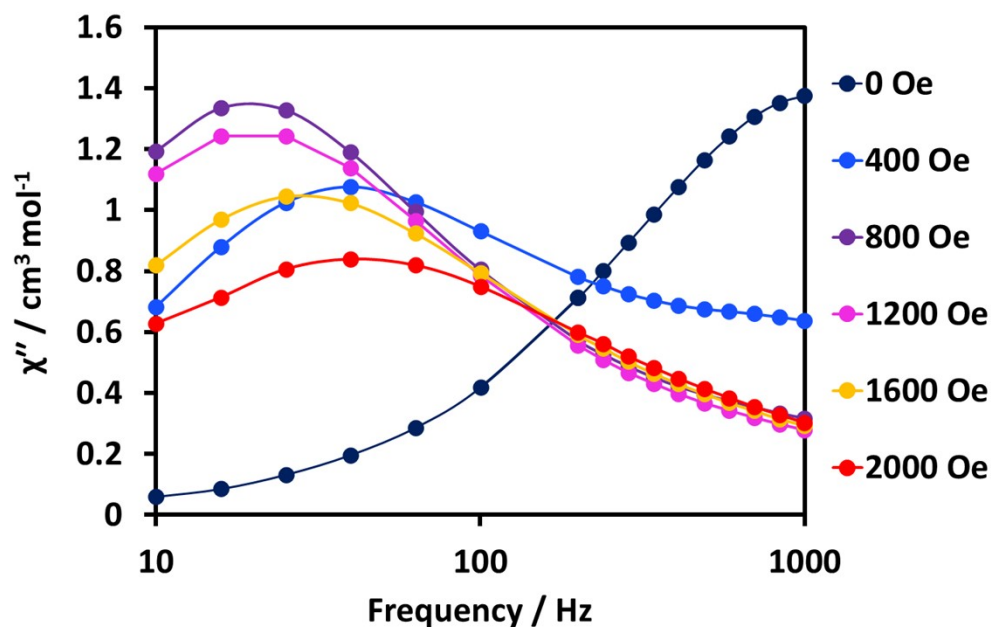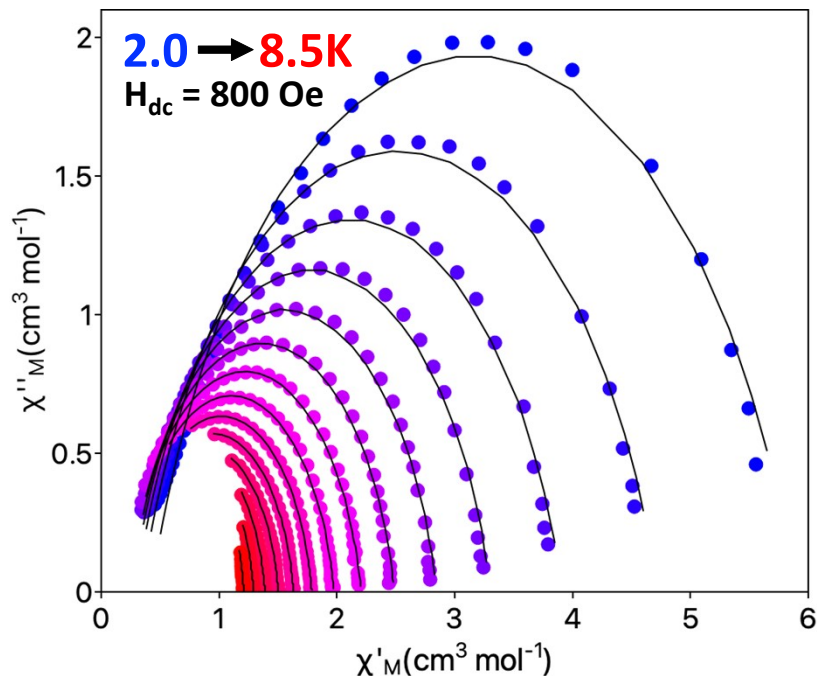
Table S8. Cole-Cole fit values of complex **1** between 1.8–5.7 K under zero applied *dc* field.

T / K	χ_S / emu mol^{-1}	χ_T / emu mol^{-1}	τ / s	α	Residual
1.8	2.27E+00	6.14E+01	6.96E-04	1.61E-01	3.37E+00
2.1	2.48E+00	4.90E+01	6.16E-04	1.32E-01	4.60E+00
2.4	2.44E+00	4.14E+01	5.64E-04	1.16E-01	4.63E+00
2.7	2.32E+00	3.54E+01	5.23E-04	1.04E-01	3.60E+00
3	2.17E+00	3.09E+01	4.87E-04	9.60E-02	2.79E+00
3.3	2.06E+00	2.73E+01	4.56E-04	8.83E-02	2.08E+00
3.6	1.91E+00	2.44E+01	4.26E-04	8.29E-02	1.57E+00
3.9	1.82E+00	2.20E+01	3.97E-04	7.67E-02	1.09E+00
4.2	1.74E+00	2.00E+01	3.68E-04	7.00E-02	7.86E-01
4.5	1.66E+00	1.83E+01	3.38E-04	6.30E-02	5.88E-01
4.8	1.57E+00	1.69E+01	3.07E-04	5.66E-02	4.04E-01
5.1	1.46E+00	1.56E+01	2.73E-04	5.05E-02	2.60E-01

T / K	χ_S / emu mol⁻¹	χ_T / emu mol⁻¹	τ / s	α	Residual
5.4	1.36E+00	1.46E+01	2.40E-04	4.41E-02	1.67E-01
5.7	1.25E+00	1.36E+01	2.08E-04	3.84E-02	1.07E-01

Table S9. Cole-Cole fit values of complex **2** between 1.8–5.7 K under zero applied *dc* field.

T / K	χ_S / emu mol⁻¹	χ_T / emu mol⁻¹	τ / s	α	Residual
1.8	2.27E+00	6.14E+01	6.96E-04	1.61E-01	3.37E+00
2.1	2.48E+00	4.90E+01	6.16E-04	1.32E-01	4.60E+00
2.4	2.44E+00	4.14E+01	5.64E-04	1.16E-01	4.63E+00
2.7	2.32E+00	3.54E+01	5.23E-04	1.04E-01	3.60E+00
3	2.17E+00	3.09E+01	4.87E-04	9.60E-02	2.79E+00
3.3	2.06E+00	2.73E+01	4.56E-04	8.83E-02	2.08E+00
3.6	1.91E+00	2.44E+01	4.26E-04	8.29E-02	1.57E+00
3.9	1.82E+00	2.20E+01	3.97E-04	7.67E-02	1.09E+00
4.2	1.74E+00	2.00E+01	3.68E-04	7.00E-02	7.86E-01
4.5	1.66E+00	1.83E+01	3.38E-04	6.30E-02	5.88E-01
4.8	1.57E+00	1.69E+01	3.07E-04	5.66E-02	4.04E-01
5.1	1.46E+00	1.56E+01	2.73E-04	5.05E-02	2.60E-01
5.4	1.36E+00	1.46E+01	2.40E-04	4.41E-02	1.67E-01
5.7	1.25E+00	1.36E+01	2.08E-04	3.84E-02	1.07E-01

Table S10. Cole-Cole fit values of complex **3** between 1.8–4.6 K under an applied *dc* field of 2000 Oe.

T / K	χ_S / emu mol⁻¹	χ_T / emu mol⁻¹	τ / s	α	Residual
1.8	1.10E+00	6.25E+00	1.69E-03	3.40E-01	8.34E-02
2.2	9.35E-01	5.47E+00	1.16E-03	3.49E-01	6.29E-02
2.6	8.28E-01	5.01E+00	7.95E-04	3.40E-01	5.83E-02
3	7.03E-01	4.58E+00	5.20E-04	3.21E-01	4.23E-02
3.4	6.19E-01	4.23E+00	3.40E-04	2.79E-01	1.98E-02
3.8	4.83E-01	3.95E+00	2.14E-04	2.34E-01	2.79E-02
4.2	2.39E-01	3.69E+00	1.29E-04	1.93E-01	2.80E-02
4.6	6.78E-07	3.47E+00	8.04E-05	1.56E-01	2.46E-02

Table S11. Cole-Cole fit values of complex **4** between 2.0-8.5 K under an applied *dc* field of 800 Oe.

T / K	χ_S / emu mol^{-1}	χ_T / emu mol^{-1}	τ / s	α	Residual
2.0	1.25E+00	1.68E+01	9.21E-03	2.11E-01	1.04E+00
2.5	1.01E+00	1.35E+01	6.11E-03	1.96E-01	5.60E-01
3.0	8.84E-01	1.12E+01	4.31E-03	1.81E-01	3.98E-01
3.5	8.04E-01	9.45E+00	3.01E-03	1.65E-01	2.83E-01
4.0	7.61E-01	8.14E+00	2.00E-03	1.48E-01	2.03E-01
4.5	7.28E-01	7.11E+00	1.24E-03	1.36E-01	1.31E-01
5.0	7.20E-01	6.31E+00	7.41E-04	1.29E-01	7.83E-02
5.5	7.46E-01	5.65E+00	4.42E-04	1.21E-01	4.39E-02
6.0	8.12E-01	5.11E+00	2.70E-04	1.10E-01	2.20E-02
6.5	8.66E-01	4.67E+00	1.68E-04	9.94E-02	1.13E-02
7.0	8.27E-01	4.30E+00	1.03E-04	9.57E-02	5.11E-03
7.5	5.73E-01	3.98E+00	5.80E-05	9.49E-02	3.52E-03
8.0	7.01E-14	3.70E+00	2.89E-05	9.69E-02	1.89E-03
8.5	9.36E-14	3.46E+00	1.81E-05	7.89E-02	1.98E-03